Posted on 23 Nov 2022 — The copyright holder is the author/funder. All rights reserved. No reuse without permission. — https://doi.org/10.1002/essoar.10500307.1 — This a preprint and has not been peer reviewed. Data may be preliminary.

Effect of fault roughness on aftershock distribution and post co-seismic strain accumulation

Khurram Aslam[1]

[1]University of Memphis

November 23, 2022

Abstract

We perform physics-based simulations of earthquake rupture propagation on geometrically complex strike-slip faults. We consider many different realization of the fault roughness and obtain heterogeneous stress fields by performing dynamic rupture simulation of large earthquakes. We calculate the Coulomb failure function (CFF) for all these realizations so that we can quantify zones of stress increase/shadows surrounding the main fault and compare our results to seismic catalogs. To do this comparison, we use relocated earthquake catalogs from Northern and Southern California. We specify the range of fault roughness parameters based on past observational studies. The Hurst exponent (H) varies in range from 0.5 to 1 and RMS height to wavelength ratio (RMS deviation of a fault profile from planarity) has values between 10-2 to 10-3. For any realization of fault roughness, the Probability density function (PDF) values relative to the mean CFF change show a wider spread near the fault and this spread squeezes into a narrow band as we move away from fault. For lower value of RMS ratio (10-3), we see bigger zones of stress change near the hypocenter and for higher value of RMS ratio (10-2), we see alternate zones of stress increase/decrease surrounding the fault to have comparable lengths. We also couple short-term dynamic rupture simulation with long-term tectonic modelling. We do this by giving the stress output from one of the dynamic rupture simulation (of a single realization of fault roughness) to long term tectonic model (LTM) as initial condition and then run LTM over duration of seismic cycle. This short term and long term coupling enables us to understand how heterogeneous stresses due to fault geometry influence the dynamics of strain accumulation in the post-seismic and inter-seismic phase of seismic cycle.

Modelling the spatio-temporal pattern of hetrogeneous stress and strain accumulation due to earthquake rupture on geometrically complex fault.

Khuram S. Aslam[1] and Eric G. Daub[1]

1 Center for Earthquake Research and Information, The University of Memphis

Why this Study?

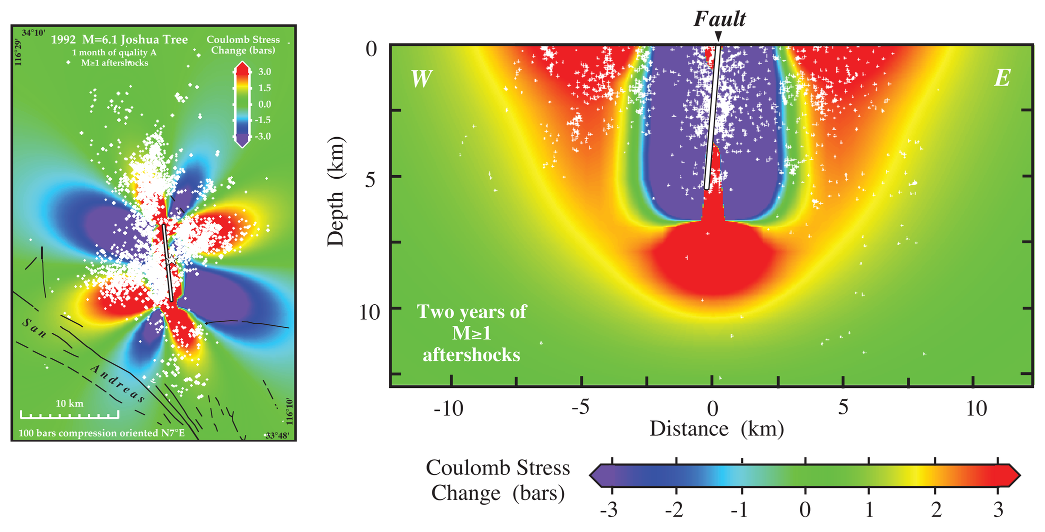

▲ Figure 1. Aftershocks distribution of Joshua Tree 1992 earthquake. Left: Map view Right: Cross-sectional view (figure taken from King et al., 1994)

Real geological faults and self affinity

(a)

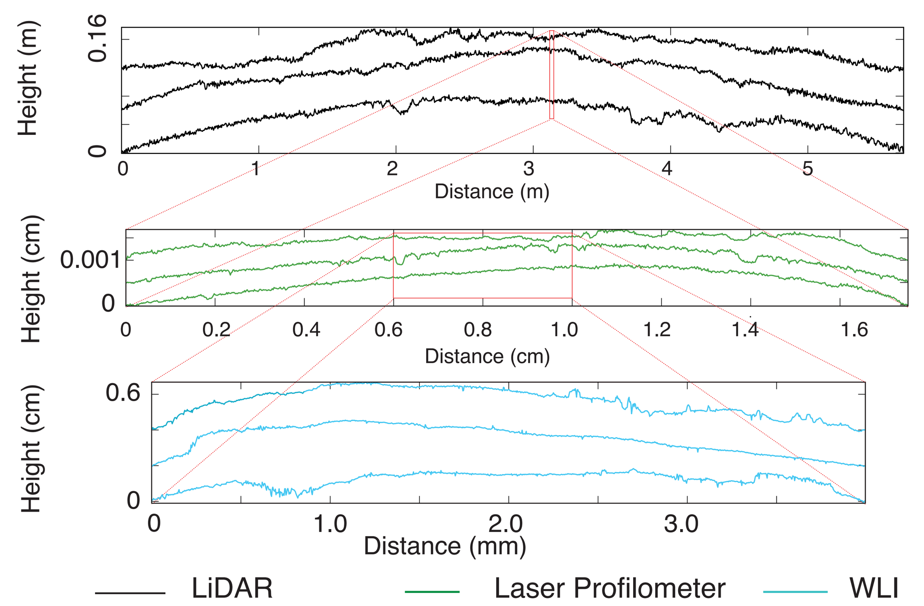

▲ Figure 2. (a) Roughness profiles from the Corona Heights fault surface in directions parallel to slip (Along slip) . A magnified portion of the profiles is also shown to observe the properties of fault profile. (Reproduced from Candela et al., 2012).

Self affine fractals:

Scaling transformation: $x \longrightarrow \beta x$, $y \longrightarrow \beta^H y$

The power spectral density: $P(k) = c\,k^{(-1-2H)}$

Self Similar fractals: Special case when $H = 1$

(b)

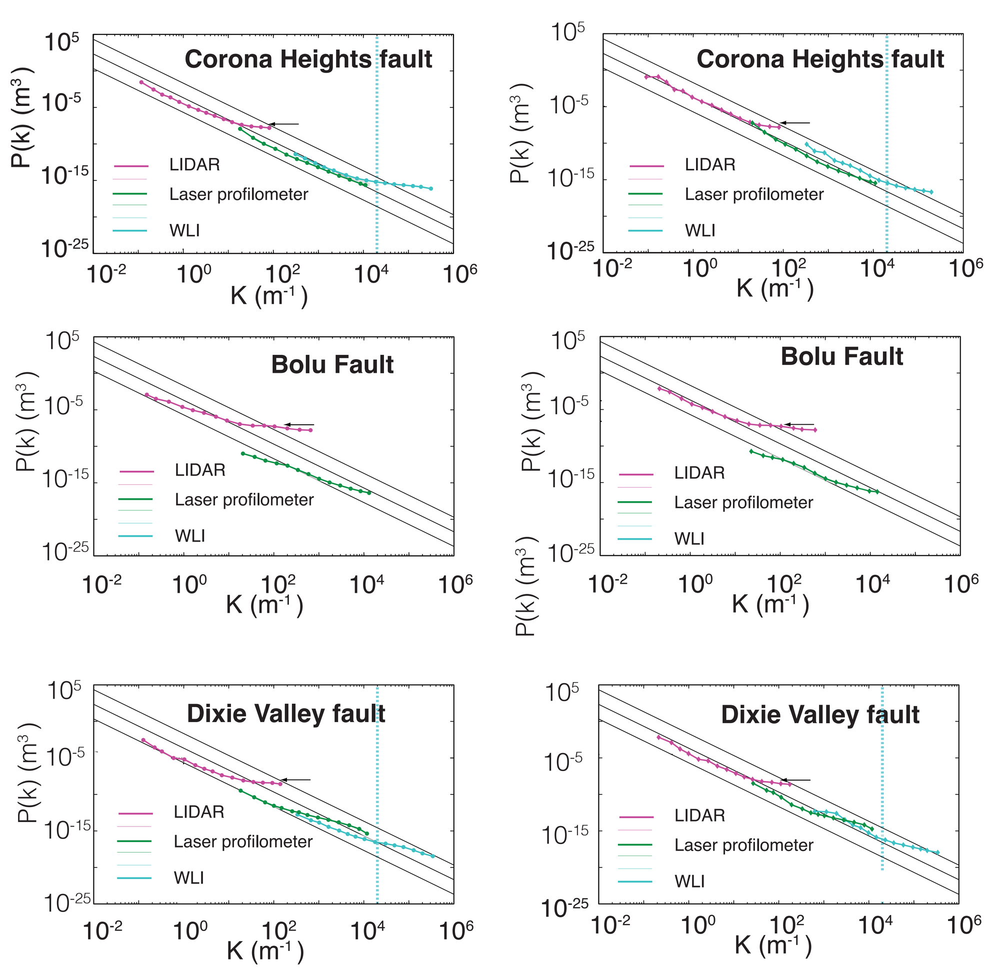

▲ Figure 1 (b) Combined Fourier power spectra from the three faults analyzed (left) along the slip direction and (right) perpendicular to it. Dark lines represent power law fits for three self-similar rough surfaces (i.e., H = 1) with RMS = 0.1 L, RMS = 0.01 L and RMS = 0.001 L from bottom to top respectively (Reproduced from Candela et al., 2012).

Methodology

We use the dynamic rupture propagation code fdfault v.1.0 written by Dr. Eric Daub to perform all simulations. This code solves elastodynamic wave equation using finite differences.

Nucleation strategies considered:

1) overstressing a certain patch length of fault. 2) overstressing a single node point.
3) Using transient slip weakening. 4) Transient overstressing.

Model Setup, friction law and modelling parameters

We used Slip weakening law to model the friction present on the fault. To represent healing on the fault after failure, we will use shear transformation zone theory in future.

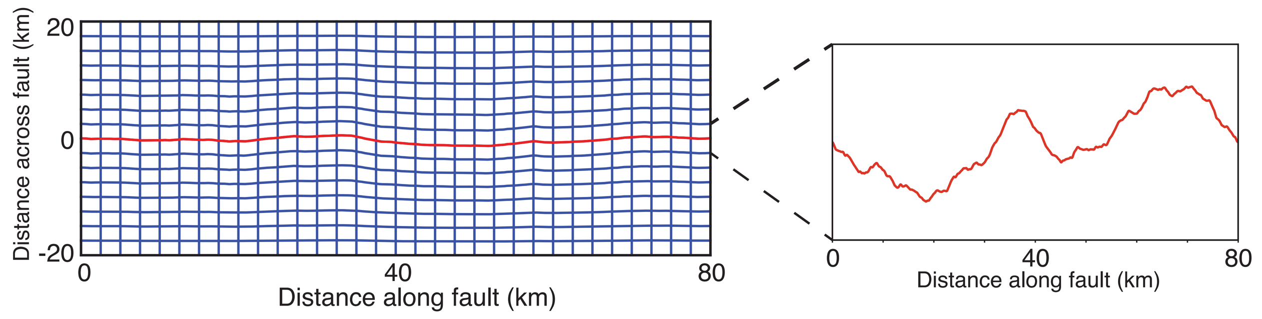

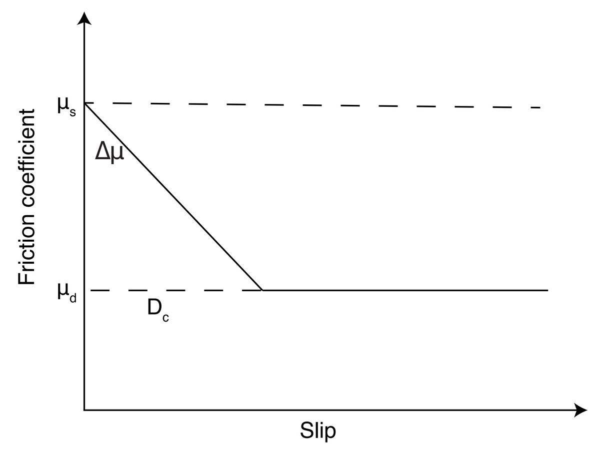

Parameters	Value
Hurst exponent	1.0-0.5
RMS ratio	0.001-0.01
X_{total} , Y_{total}	80 km , 40 km
Vp,Vs	6 , 3.464 km/sec
ρ	2.67 g/cm^3
λ= G	32.04 GPa
Δx= Δy	25 m
Δμ, Dc	0.5 , 0.4 cm

▲ Figure 3. Top: Model setup. All simulations have same setup with similar modelling parameters but different fault profile. Bottom: The slip weakening law; A static frictional coefficient drops to dynamic value over a crictical slip distance.

Simulations Plan

Table 1. Simulations plan indicating some of the important simulations that have been completed already.

	Hurst exponent			RMS ratio		Material property		Friction law		Nucleation		Realizations	
	1.0	0.8	0.6	0.01	0.001	Elastic	Plastic	SW	STZ	Patch	Other	1	100
S1	x			x		x		x		x			x
S2		x			x	x		x			x	x	
S3			x	x		x		x		x			x
S4	x			x			x	x		x		x	
S5	x			x		x		x			x	x	
S6	x				x	x		x		x			x
S7		x			x	x		x		x			x

Results

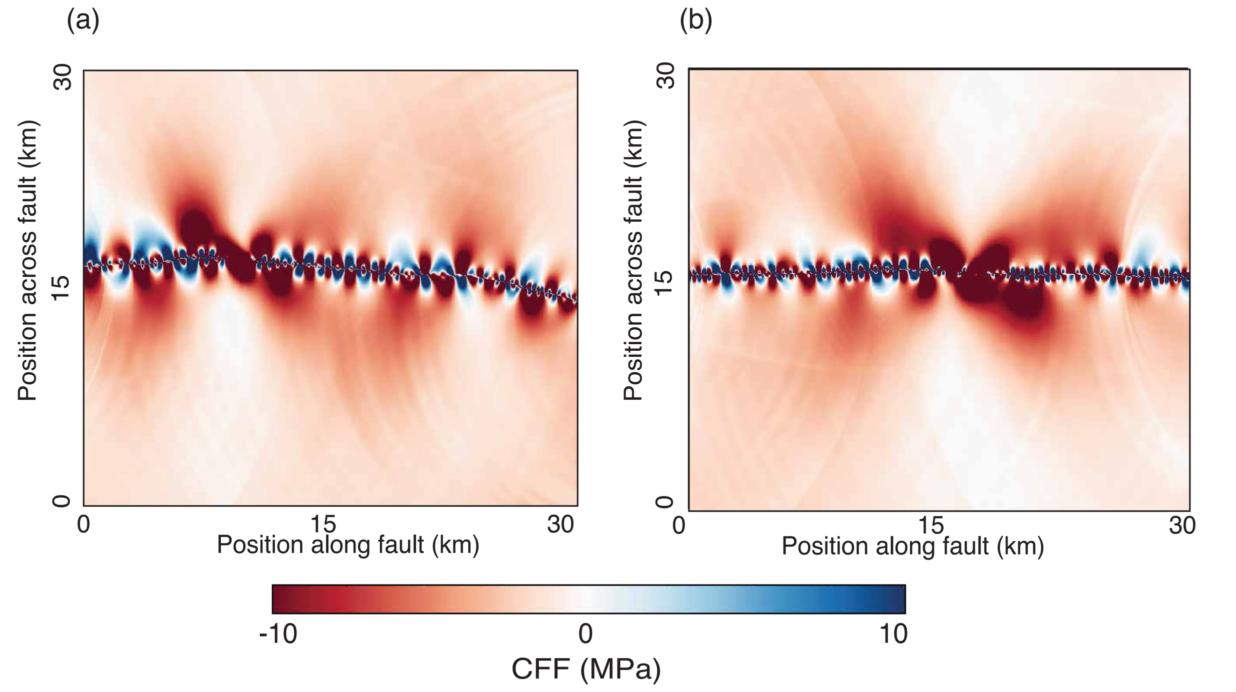

▲ Figure 4. (a) CFF of a single realization of rough fault with RMS ratio of '0.01' and H value of '1'. (b) CFF of a single realization of rough fault with RMS ratio of '0.01' and H value of '0.6'.

Results - continued

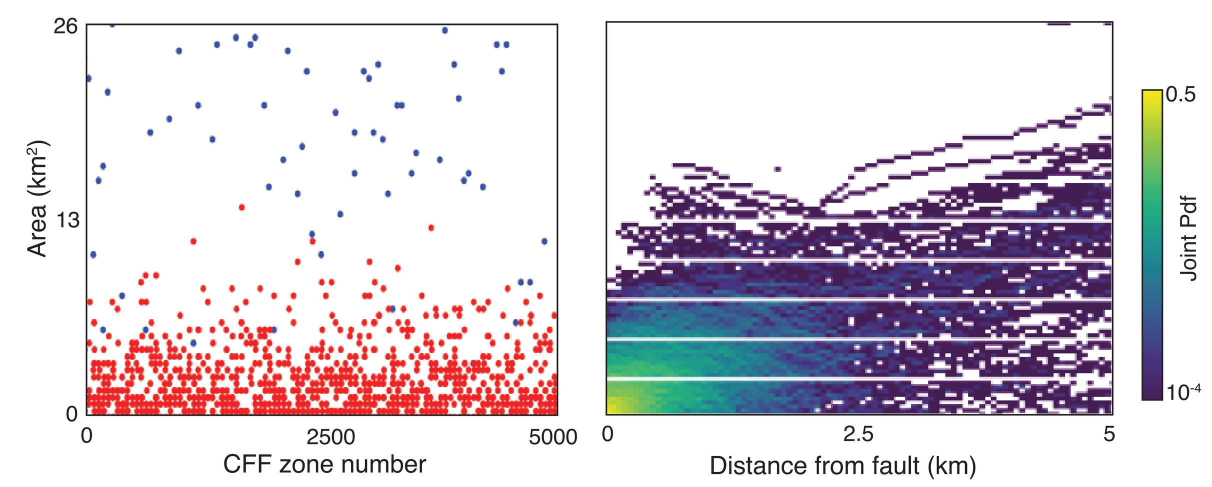

▲ Figure 5. (a) Positive CFF zones and their respective areas at different distances. Red color shows distance of 1 km while blue shows 5 km distance. (b) Joint pdf of positive CFF zones with a certain area and distance from fault. (RMS=0.01 and H=0.6)

(c)

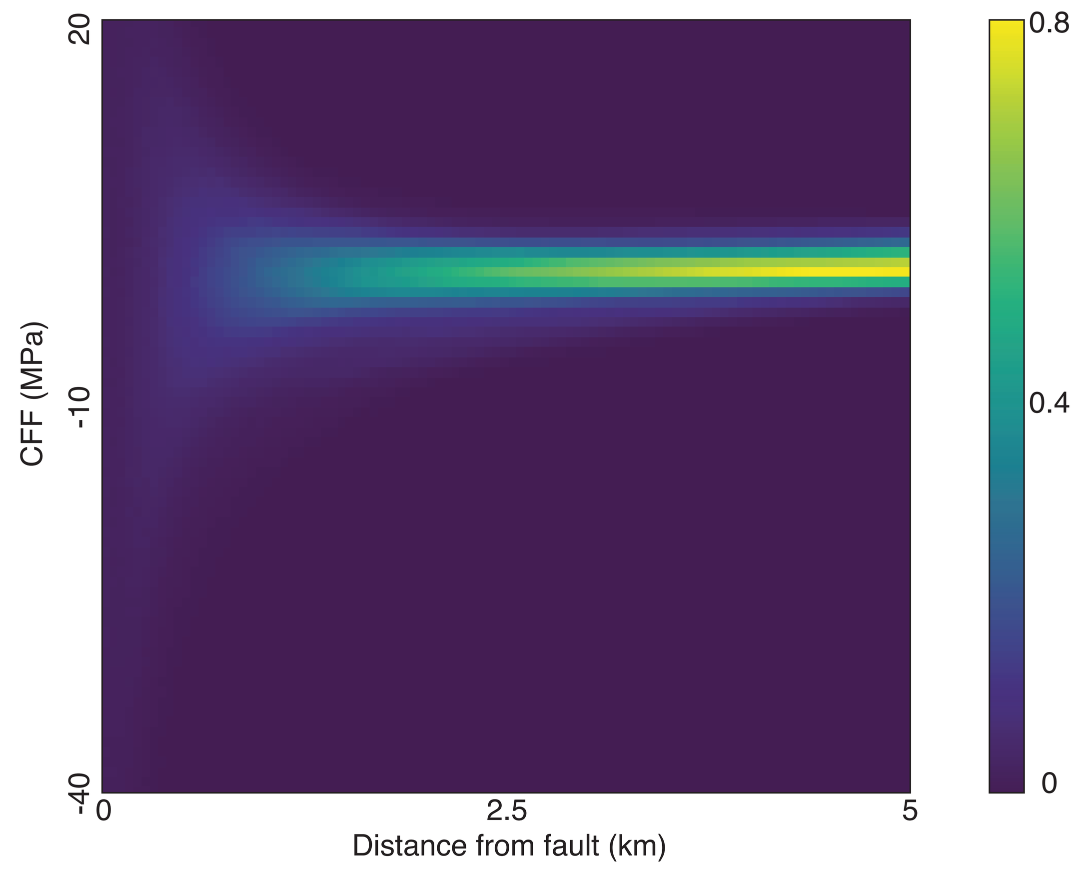

▲ Figure 5. (c) CFF vs distance plot. The color represents(PDF values relative to the mean CFF. This plot is made using 100 realization of a rough fault with RMS ratio of '0.01' and H value of '1.0'.

Available Data

1) Northern and Southern California EQ Catalog 2) Slip inversions through SRCMOD. [Shearer et al., 2005, Waldhauser and Schaff, 2008, Mai and Thingbaijam, 2014].

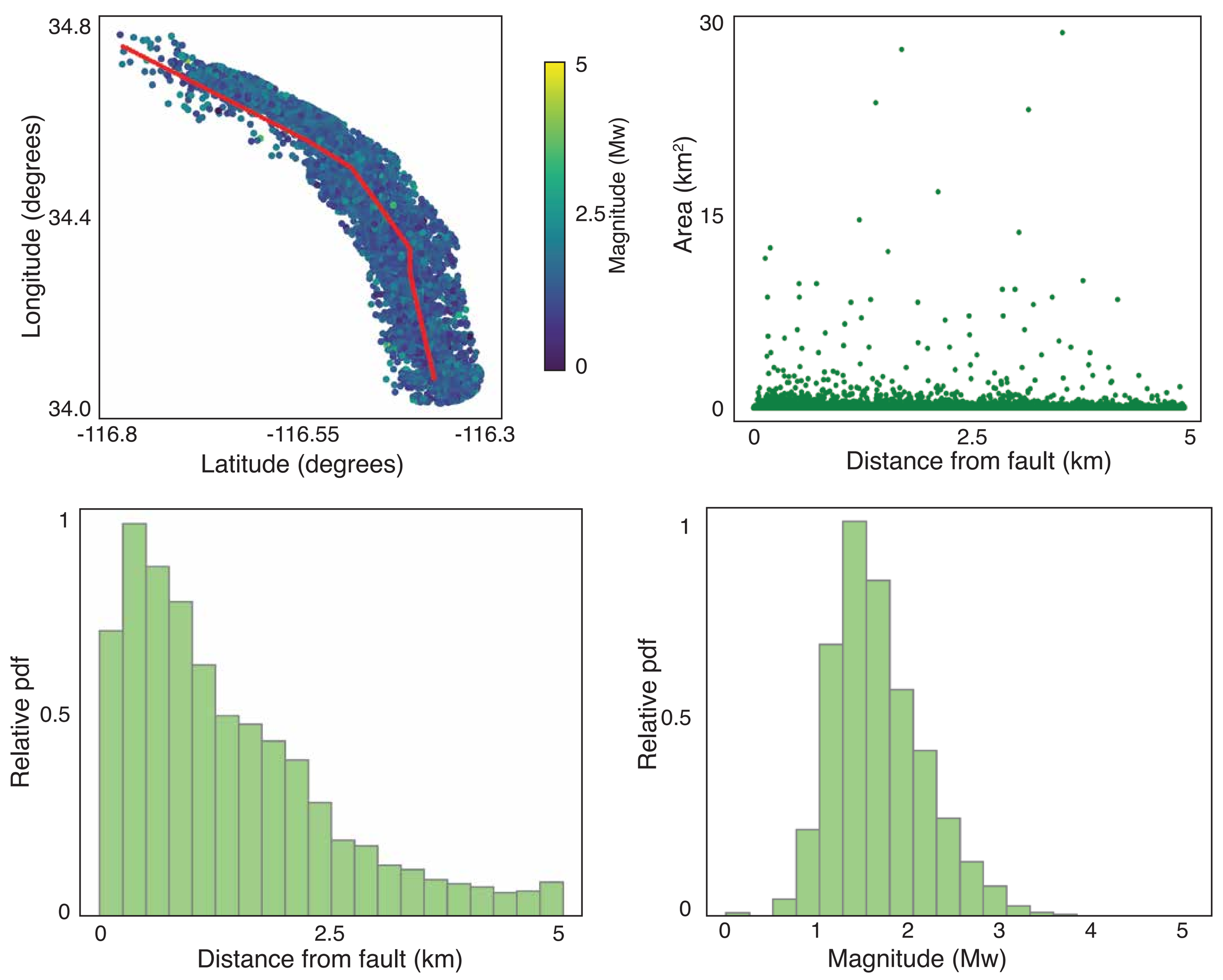

▲ Figure 6. Real aftershocks data of Loma prieta 1989 earthquake. Only those aftershocks are taken into consideration that have a distance less than 5 km from main fault rupture.

Results - continued

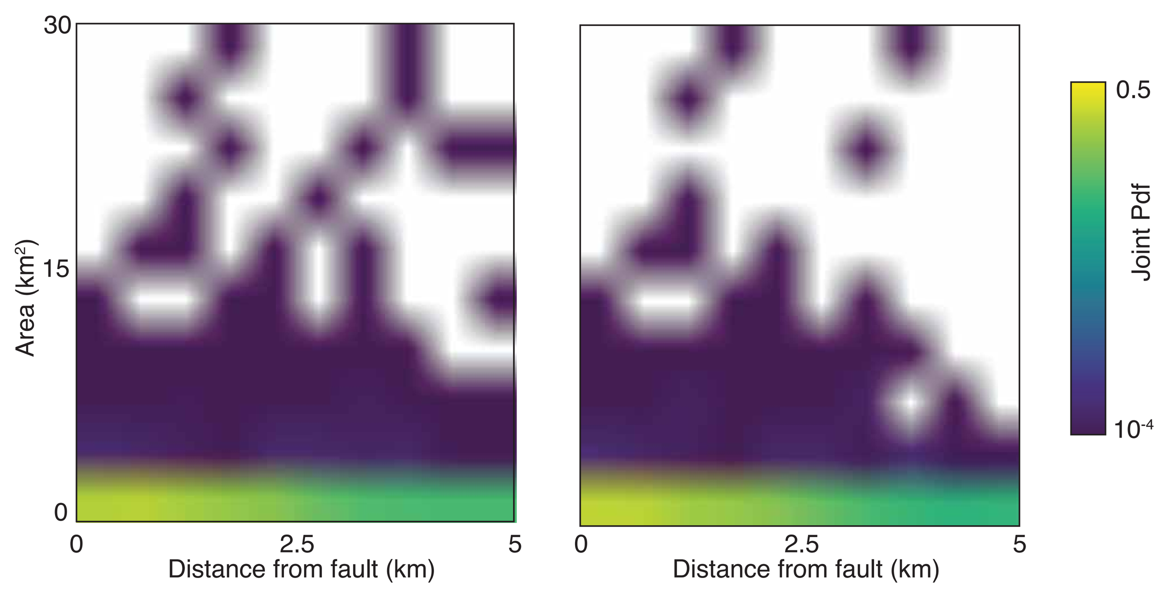

▲ Figure 7. Joint pdf of Real quakes with certain rupture area and distance away from ruptured fault. (a) Combined aftershocks data (b) Combined fore-shocks data.
Combined aftershocks and foreshocks data compiled from (1984 Morgan Hill EQ, 1989 Loma prieta EQ, 1992 Landers EQ,1994 Northridge EQ and 1999 Hector-mine EQ).

Coupling Short-term long-term dynamics

We have coupled our short-term rupture dynamics code with the LTM. The LTM code DynEarthSol3D is a finite element code that solves the momentum balance and the heat transfer equation in Lagrangian form using unstructured meshes.

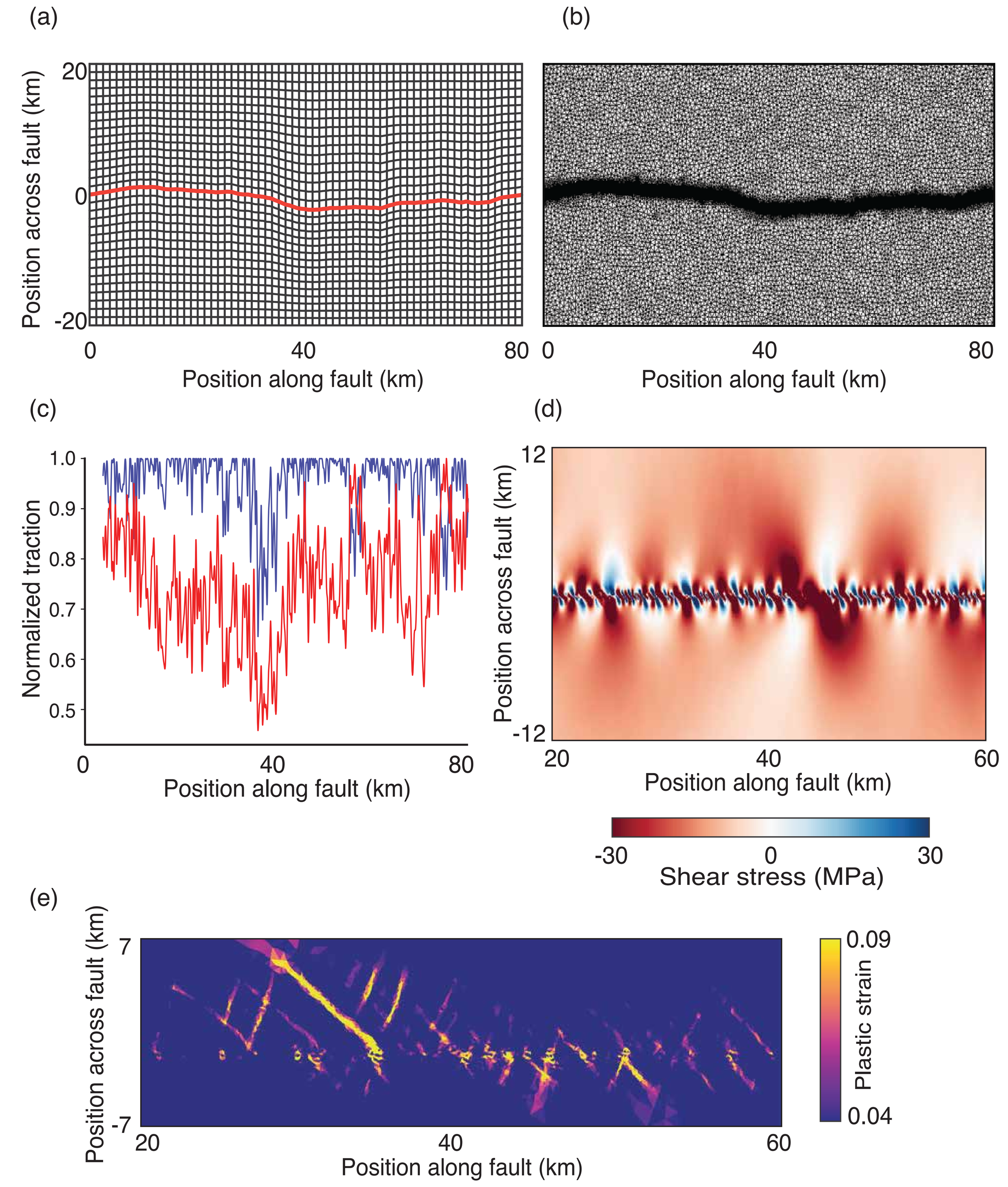

▲ Figure 8. Coupling short-term long-term models. (a) Dynamic rupture simulation grid with self-similar fault profile . (b) LTM mesh with initial fault zone extracted automatically. (c) Tractions on the fault. Shear (blue) and normal(Red) traction values vary a lot due to geometry of the fault. (d) Shear stress across fault after seismic waves have propogated away (this is the intial condition for LTM model) . (e) Plastic strain developed after couple of days. A highly damage zone is visible across the fault with develoment of new fractures.

Acknowledgements

This work was supported by the Southern California Earthquake Center (SCEC) through the award 17182. This research was possible thanks to support from the Center for Earthquake Research and Information (CERI) at the University of Memphis. CERI is designated as a Center of Excellence by the Tennessee Board of Regents and is funded in part by the State of Tennessee under State Sunset Laws (SB 1510 and HB 1608, 2015–2016). For all computational work, we used the University of Memphis High Performance Computing Center, housed at the FedEx Institute of Technology.